G-Protein–Effector Coupling: A Real-Time Light-Scattering Assay for Transducin–Phosphodiesterase Interaction†

Martin Heck and Klaus Peter Hofmann*

Institut für Biophysik und Strahlenbiologie, Albertstrasse 23, 79104 Freiburg, FRG

Received March 1, 1993; Revised Manuscript Received May 17, 1993

ABSTRACT: We describe a real-time assay for the interaction of the G-protein of retinal rods, transducin (G_t), with its effector, cGMP phosphodiesterase (PDE). The purified proteins were recombined with isolated rod disk membranes. Reactions were triggered by flash photolysis of the receptor rhodopsin, and monitored by changes of near-infrared light scattering (LS signals). PDE-related LS signals from membrane preparations have been described by others [Caretta, A., & Stein, P. J. (1986) *Biochemistry 25*, 2335–2341; Bennett, N., & Clerc, A. (1992) *Biochemistry 31*, 1858–1866]. In the present study, the previous overall light-scattering (turbidity) approach was improved by a specific optical setup and millisecond time resolution. This allowed isolation of a fast "PDE signal" which monitors G_t–PDE interaction on the membrane and in real time. The assignment to the reaction is made by the following observations: (i) preactivation of PDE by purified $G_\alpha GTP\gamma S$ gradually suppresses the signal; (ii) the peak amplitude of the signal is stoichiometric with respect to both G_t and PDE; and (iii) the rise and delay time fit into a kinetic model for a reaction of activated G_t (G*). A comparative investigation, relating the PDE signal with G_t activation and PDE enzymatic activity, led to the following results: (i) the apparent dissociation constant for the interaction of G* with the first binding site on membrane-bound PDE is less than 2.5 nM; (ii) the time interval between formation of G* and its interaction with PDE is less than 5 ms; (iii) membrane-bound PDE, even in its preactivated form, slows the release of G* from the membrane. The results suggest a kinetic competition mechanism in which activated G_t stays long enough on the membrane to favor its capture by the PDE. The 5-ms time it takes G* to couple to PDE *in vitro* fits well into the time frame for this reaction, as determined *in situ* by electrophysiology.

Photoexcitation of rod photoreceptors involves the sequential activation of rhodopsin (R), transducin (G_t),[1] and cGMP phosphodiesterase (PDE) on the disk membranes of the rod outer segment. Absorption of light transforms rhodopsin into the activated form of the receptor (R*), which interacts with G_t to catalyze the exchange of GTP for GDP in the nucleotide binding site. GTP-bound transducin dissociates from the catalytic complex and represents the active signaling form of G_t (G*). Released R* is free to activate further molecules of G_t, resulting in amplification of the light signal. The next step in the transduction cascade is the interaction of G* with the effector PDE. By contrast with the catalytic R*–G interaction, the activation of PDE results from the binding of G* which renders the PDE hydrolytically active. The resulting drop in cGMP concentration directly closes the cGMP-regulated channels in the plasma membrane, leading to hyperpolarization and neuronal signaling [for reviews, see Stryer (1986), Liebman et al. (1987), and Chabre and Deterre (1989)].

The PDE holoenzyme is heterotrimeric (Baehr et al., 1979), with two catalytic subunits, PDE_α and PDE_β, inhibited by two small subunits (PDE_γ or I) in the dark latent state of the enzyme (Deterre et al., 1988; Whalen & Bitensky, 1989; Fung et al., 1990). Catalytic R*–G_t interaction requires the G_t heterotrimeric holoprotein [reviewed in Chabre and Deterre (1989) and Hofmann (1993)], while the GTP-bound α-subunit alone is competent to activate the PDE (Fung et al., 1981; Wensel & Stryer, 1986; Deterre et al., 1986). It does so by relieving the inhibitory effect of the PDE_γ-subunit (Hurley & Stryer, 1982; Yamazaki et al., 1982). It is known that two active G_α molecules are required to fully activate one molecule of PDE (Deterre et al., 1988; Whalen & Bitensky, 1989; Fung et al., 1990). However, the intermediate states of the activation process are still unclear, including the relative activity of the 1:1 G*PDE complex (Deterre et al., 1988; Whalen & Bitensky, 1989; Bennett & Clerc, 1989; Wensel & Stryer, 1990) and possible cooperativity (Whalen & Bitensky, 1989; Bennett & Clerc, 1989).

The variety of subunit interactions in this system is not the only problem in studying the PDE activation mechanism. Additional complexity is introduced by the membrane binding behavior of the visual proteins. They are membrane-bound as all their fellow proteins in other G-protein-coupled transduction systems, with the receptor as an intrinsic membrane protein. In the rod photoreceptor, G_t and PDE are bound to be the disk membrane surface by weak interactions that may involve ionic and hydrophobic forces. In preparations of disrupted and diluted rod outer segments (ROS) or of isolated membranes reconstituted with the proteins, a significant fraction of G_t and PDE is found in solution, and the activated G_α-subunit even behaves as a freely soluble protein (Kühn, 1984). On the other hand, the activated G*PDE complex binds to the membrane with high affinity (Malinski & Wensel, 1992; Catty et al., 1992).

Several techniques are available to analyze PDE activation, including the cGMP hydrolysis proton assay (Liebman & Pugh, 1979; Liebman & Evanczuk, 1982), the heat production

† This work was supported by grants from the Deutsche Forschungsgemeinschaft (SFB 60, H-5, to K.P.H.).

[1] Abbreviations: ROS, rod outer segment(s); PDE, rod cGMP phosphodiesterase, $PDE_{\alpha\beta\gamma\gamma}$; R*, photoexcited rhodopsin; G_t, rod G-protein, transducin, $G_{\alpha\beta\gamma}$; G*, light-activated transducin; $G_\alpha GTP\gamma S$, $GTP\gamma S$-bound α-subunit of transducin; $GTP\gamma S$, guanosine 5′-*O*-(3-thiotriphosphate); HEPES, *N*-(2-hydroxyethyl)piperazine-*N*′-2-ethanesulfonic acid; LS, light scattering; PIPES, piperazine-*N*,*N*′-bis(2-ethanesulfonic acid); Tris, tris(hydroxymethyl)aminomethane; PMSF, phenylmethanesulfonyl fluoride; DTT, dithiothreitol.

0006-2960/93/0432-8220$04.00/0

assay (Vuong & Chabre, 1991), or direct binding assays using fluorescence labels (Wensel & Stryer, 1990; Erickson & Cerione, 1991; Artemyev, 1992). For such a complex system, kinetic light scattering can be useful as a complementary approach, since it probes an endogenous physically predominant step in a complicated sequence of events and measures exclusively the membrane-bound interaction mode. Adequate kinetic resolution separates the activating reactions of the visual cascade from postponed steps (e.g., the GTPase reaction). A well-studied example is the dissociation signal (Kühn et al., 1981) which monitors G_t activation in real time by probing its fast release from the membrane (Schleicher & Hofmann, 1987).

The subject of this study is a "PDE signal", which monitors the transduction step subsequent to G_t activation. This type of signal was already described as the fast part of a PDE-related more complex turbidity change ["phosphodiesterase activation signal" (PAS); Bennett, 1986; Bennett & Clerc, 1992].

The experiments allow the conclusion that flash-activated G_t can bind to PDE before it has a chance to escape into solution, even in the highly diluted system used. Thus, the reaction can proceed *in vitro* with the kinetics predicted from *in situ* measurements of the electrical response (Cobbs & Pugh, 1987).

EXPERIMENTAL PROCEDURES

Washed Disk Membranes. Washed disk membranes were prepared as described (Kahlert et al., 1990). About 60 bovine retinas were collected in 1 mL per retina of 21% sucrose in 10 mM PIPES (pH 7.2), 130 mM NaCl, 1 mM $CaCl_2$, 0.5 mM $MgCl_2$, 0.5 mM EDTA, 1 mM DTT, and 0.1 mM PMSF (buffer A) and stored at –80 °C until use. Thawed retinas were vortexed for 30 s and filtered through a 100-μm nylon-mesh. The suspension was layered upon a 36% sucrose cushion and centrifuged (48000*g*, 30 min, 4 °C). The floating ROS were washed once (12000*g*, 20 min, 4 °C) and centrifuged on a continuous (25–42%) sucrose gradient (90000*g*, 60 min, 4 °C). The ROS were collected and washed again in buffer A (12000*g*, 20 min, 4 °C). The pellet was suspended twice in 5 mM PIPES (pH 7.0), 1 mM EDTA, and 1 mM DTT (buffer B) and centrifuged (48000*g*, 30 min, 4 °C). The final pellet was suspended in a small volume of buffer A and stored at –80 °C. This preparation yields membranes stripped of peripheral proteins and of variable osmotic activity; electron micrographs show mostly disrupted membranes. Similar PDE signals were seen with fractions of this preparation, selected for high or low osmotic activity by the floating procedure of Smith et al. (1975), or with the vesicle preparation according to Bauer (1988).

Transducin and PDE. About 80 bovine retinas were collected in 1 mL per retina of 42% sucrose in 10 mM Tris (pH 7.5), 100 mM NaCl, 5 mM $MgCl_2$, 1 mM DTT, 0.1 mM PMSF, 5 μM leupeptin, and 0.1 μM aprotinin (buffer C) and shaken for 3 min. The suspension was centrifuged (6000*g*, 5 min, 4 °C). The floating ROS were filtered through a cotton tissue, washed once with buffer C (7000*g*, 8 min, 4 °C), and centrifuged on a continuous (25–42%) sucrose gradient (90000*g*, 60 min, 4 °C). The ROS were collected, washed in 21% sucrose in buffer C (12000*g*, 20 min, 4 °C), and stored at –80 °C. Thawed ROS were homogenized and washed twice in buffer C (12000*g*, 20 min, 4 °C). Crude PDE was obtained by two low ionic strength extractions with 2 mM Tris (pH 7.5), 0.4 mM $MgCl_2$, 0.1 mM EDTA, 1 mM DTT, 0.1 mM PMSF, 5 μM leupeptin, and 0.1 μM aprotinin (buffer D) of the illuminated membranes, and transducin was obtained by subsequent extraction of the membranes with 100 μM GTP in buffer D.

Purification of crude PDE was done as described by Baehr et al. (1979). Briefly, the crude extract was concentrated by ultrafiltration (Amicon, YM-30) and chromatographed on a DEAE-52 column (0.9 × 4 cm). Elution was carried out with a linear NaCl gradient (100–250 mM) in 20 mM Tris, pH 7.5, 1 mM DTT, and 0.1 mM EDTA (buffer E). Fractions containing PDE were concentrated, dialyzed against 10 mM PIPES, pH 7.2, 100 mM NaCl, 5 mM $MgCl_2$, and 1 mM DTT (buffer F) and further purified by gel filtration (G 100–120). Aliquots were stored in buffer F at –40 °C.

Protein concentrations were determined by the method of Bradford (1976) using bovine serum albumin as the standard.

$G_\alpha GTP\gamma S$. $G_\alpha GTP\gamma S$ was prepared like transducin using 20 μM $GTP\gamma S$ instead of GTP, concentrated by ultrafiltration (Amicon, YM-10), and washed with buffer F. The different subunits were separated by affinity chromatography (Blue Sepharose CL-6B). $G_\alpha GTP\gamma S$ was eluted with 900 mM NaCl in buffer F, concentrated, dialyzed against buffer F, and stored at –40 °C.

Light-Scattering Measurements. Light-scattering changes (LS signals) were measured in a setup similar to the one previously used by Schleicher and Hofmann (1987). The technique employs a continuous 840-nm incident light beam from a light-emitting diode (Hitachi HLP 60R). Scattered light was collected by Fresnel lens optics within angular range 16 ± 2° and focused on a solid-state photodetector (Centronics OSD 100 5-T). LS signals were recorded with 1-ms dwell time of the A/D converter (Nicolet 4096); the cutoff frequency was set to 1 kHz. LS signals were induced by photolysis of rhodopsin with a green flash (20 μs), attenuated by appropriate neutral density filters. Unless otherwise indicated, samples were prepared in buffer F, in a final volume of 300 μL, in a 10-mm path cuvette. Proteins were added as indicated in the figure legends. Experiments were performed at room temperature (19 ± 1 °C). To suppress base-line activation, 2.5 mM NH_2OH was added to the samples during incubation (30 min). In the range of the scattering angle used, the PDE signal dominates other scattering signals, including the dissociation signal. Addition of purified PDE to suspensions of washed disk membranes in the dark induced a large increase (up to 45%) of the scattered light. No scattering change was observed upon addition of trypsin-treated PDE, even when the tryptic digestion was too short to fully activate the enzyme. It is known that cleavage of membrane attachment sites precedes activation of PDE by trypsin (Ong et al., 1989; Catty & Deterre, 1991). Thus, the slow scattering change is most likely related to the reassociation of PDE with the disk membranes.

Measurement of PDE Activity. PDE activity was determined by measuring proton release due to cyclic GMP hydrolysis with a pH electrode. All assays were carried out at room temperature (19 ± 1 °C) in a final volume of 200 μL and in a buffer containing 7.5 mM HEPES (pH 7.8), 130 mM NaCl, 5 mM $MgCl_2$, 2.5 mM NH_2OH, 0.5 mM GTP, and 3 mM cGMP; protein components were added as indicated in the figure legends. The reactions were started with the same flash arrangement as used in the LS experiments. PDE activity was determined as the first time derivative of the pH records.

Data Analysis. For reasons outlined in the subsequent section, we assume for the binding of activated transducin

(G*) to PDE, as monitored by the PDE signal, a simple bimolecular reaction:

$$G^* + PDE \rightleftharpoons G^*PDE \quad (1)$$

with

$$[G^*PDE] = \frac{1}{K_D}[G^*][PDE] \quad (2)$$

where [G*], [PDE], and [G*PDE] represent the molar concentrations of G*, PDE, and G*PDE, respectively, and K_D is the apparent dissociation constant of the G*PDE complex. In addition, the following conservation relations are given:

$$[PDE]_{tot} = [PDE] + [G^*PDE] \quad (3)$$

$$[G^*]_{tot} = [G^*] + [G^*PDE] \quad (4)$$

$[PDE]_{tot}$ and $[G^*]_{tot}$ are the total concentrations of PDE and G*, respectively. Since only the membrane-associated fraction of added transducin (G_{mb}) is activated fast enough to contribute to the PDE signal (see Results), eq 4 can be replaced by

$$\rho[G]_{tot} = [G^*] + [G^*PDE] \quad (5)$$

where $[G]_{tot}$ represents the total concentration of added transducin and ρ is a scaling factor that accounts for the unknown mole fraction (relative to $[PDE]_{tot}$) of activatable and membrane-associated transducin. Therefore

$$[G^*PDE] = \frac{1}{K_D}(\rho[G]_{tot} - [G^*PDE])([PDE]_{tot} - [G^*PDE]) \quad (6)$$

This gives a quadratic equation for [G*PDE] with the solution

$$[G^*PDE] = \frac{-b \pm \sqrt{b^2 - 4ac}}{2a} \quad (7)$$

where $a = 1$, $b = -(K_D + \rho[G]_{tot} + [PDE]_{tot})$, and $c = \rho \cdot [G]_{tot}[PDE]_{tot}$.

PDE signals were separated from slower components (see Figure 1A,a) by multiexponential least-squares fit of each record. Equation 7 was used to model the relative amplitudes ($\Delta I/I$) of the PDE signal arising from the titration with transducin. A scaling factor (σ) relates the measured values to corresponding concentration units ($\Delta I/I = \sigma[G^*PDE]$). σ varies between preparations by ±50%.

The data obtained from suppression of the PDE signal by preactivation of the PDE with $G_\alpha GTP\gamma S$ were fitted with a modified eq 7:

$$\frac{[G^*PDE]}{[PDE]_{tot}} = 1 - \frac{-b' \pm \sqrt{b'^2 - 4ac'}}{2a[PDE]_{tot}} \quad (8)$$

where $a = 1$, $b' = -(K_D + \rho'[G_\alpha GTP_\gamma S]_{tot} + [PDE]_{tot})$, and $c' = \rho'[G_\alpha GTP\gamma S]_{tot}[PDE]_{tot}$.

In all fits, $[PDE]_{tot}$ was fixed, and K_D, ρ, and σ were allowed to vary.

RESULTS

A Fast Light-Scattering Signal That Depends on Transducin and PDE (PDE Signal). Figure 1A,b and Figure 1B,b show a typical dissociation signal (Kühn et al., 1981) on different time scales, evoked in a suspension of washed disk membranes by a weak flash, and in the presence of GTP and purified transducin. Previous work has established that this signal is due to the release of the light-activated transducin (G*) from the isolated membranes (Schleicher & Hofmann, 1987).

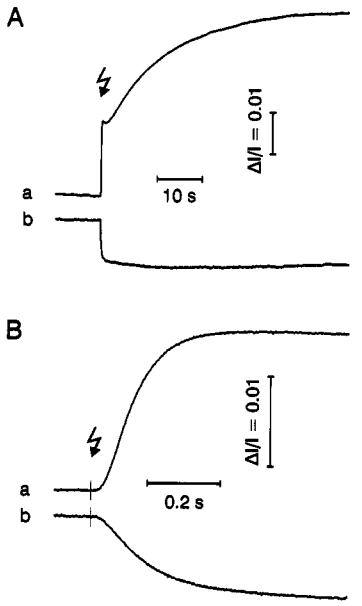

FIGURE 1: Definition of the PDE signal. Flash-induced near-infrared light-scattering changes were measured on suspensions of washed disk membranes reconstituted with purified transducin with or without purified PDE. (A) Scattering change in the presence of 0.1 μM purified PDE (a) and in the absence of PDE (b). (B) Scattering changes measured under identical conditions on an expanded time scale: (a) typical PDE signal (0.1 μM purified PDE); (b) typical dissociation signal (no PDE). Measuring conditions: 3 μM rhodopsin, mole fraction of flash-excited rhodopsin $R^*/R = 2 \times 10^{-3}$, 0.3 μM transducin, 500 μM GTP, room temperature.

When purified PDE is added to an otherwise identical sample, the same flash evokes a different light-scattering change. It extends over a longer time scale (Figure 1A,a), with complex kinetics (Caretta & Stein, 1986; Bennett & Clerc, 1992). On a short time scale, a fast signal of positive polarity can be clearly separated (Figure 1B,a). This signal we shall term "PDE signal", anticipating its detailed stoichiometric and kinetic analysis. Available data identify it with the fast phase reported in previous phosphodiesterase-dependent turbidity investigations (Bennett & Clerc, 1992; note that turbidity changes are of opposite polarity). When PDE but no transducin is added to membranes, a weak flash does not evoke any scattering change. This shows that the presence of disk membrane, receptor, G-protein, and effector is necessary and sufficient for the signal to occur.

It is important to note that only the fraction of transducin that is present on the membranes at the time of the flash is monitored in both the dissociation signal and the PDE signal. Generally, the slower binding and activation of the soluble fraction are not reflected in light scattering on the short time scale (Figure 1B) used throughout this study (Schleicher & Hofmann, 1987).

Preactivation of PDE by $G_\alpha GTP\gamma S$ Suppresses the PDE Signal. Membrane-associated PDE can be activated by purified $G_\alpha GTP\gamma S$ (Fung et al., 1981; Wensel & Stryer, 1986; Deterre et al., 1986). If the PDE signal is due to interaction of light-activated transducin (G*) with PDE, it must be suppressed by preactivation of PDE with $G_\alpha GTP\gamma S$ in the dark, prior to the flash (Wagner et al., 1987), since $G_\alpha GTP\gamma S$ competes with G* for PDE.

Figure 2 shows the dependence of the PDE signal on $G_\alpha GTP\gamma S$. Preactivation of PDE by increasing concentrations of $G_\alpha GTP\gamma S$ gradually reduces the amplitude of the PDE signal (Figure 2, inset). The more the PDE signal is reduced, the more it is replaced by a negative slower scattering change. In the absence of $G_\alpha GTP\gamma S$, the pool of G* binds to

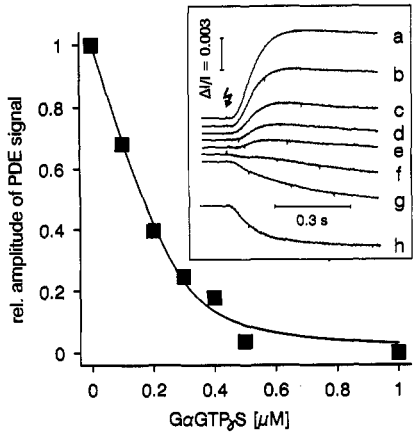

FIGURE 2: Inhibition of the PDE signal by purified by $G_\alpha GTP_\gamma S$. Amplitudes of the signals (filled squares) are normalized to the amplitude of the signal with no $G_\alpha GTP_\gamma S$ added. The solid line is a fit according to eq 8 (see Data Analysis), yielding a dissociation constant for the $G_\alpha GTP_\gamma S$–PDE interaction of $K_D = 8 \pm 4$ nM (SEM) and a mole fraction of active $G_\alpha GTP_\gamma S$ of $\rho' = 0.35$. Inset: Light-induced scattering changes in the presence of 0 (a), 0.1 (b), 0.2 (c), 0.3 (d), 0.4 (e), 0.5 (f), and 1 μM (g) $G_\alpha GTP_\gamma S$; (h) control without PDE. Note that the rise time of the dissociation signal in the presence of PDE and 1 μM $G_\alpha GTP_\gamma S$ ($t_{1/2}$ = 0.3 s) is markedly slower than the control without PDE ($t_{1/2}$ = 0.1 s). The amplitude data points were obtained by reading each signal amplitude after 340 ms, where the maximal amplitude of the PDE signal occurs in trace a. These values were then corrected by the corresponding dissociation signal amplitudes, using a linear interpolation for the dissociation signal amplitude between trace a (zero amplitude) and trace g (amplitude after 340 ms). Measuring conditions: 3 μM rhodopsin (washed membranes), flash excitation $R^*/R = 2 \times 10^{-3}$, 0.2 μM transducin, 0.1 μM PDE, 500 μM GTP.

membranous PDE and gives rise to a full control PDE signal (Figure 2a). Increasing occupation of the binding sites on PDE by added $G_\alpha GTP\gamma S$ leads to increasing G* dissociation from the membranes and is reflected in an increasing dissociation signal. When all binding sites at membranous PDE are occupied by $G_\alpha GTP\gamma S$, a dissociation signal is seen (Figure 2g) which exhibits the same final amplitude as in the absence of any PDE (Figure 2h). This indicates that, in both these cases, the same amount of transducin is released from the membranes.

However, the dissociation signal in the presence of PDE and $G_\alpha GTP\gamma S$ is markedly slower than the one without PDE. Neither purified $G_\alpha GTP\gamma S$ alone nor trypsin-activated PDE has an effect on the dissociation signal (data not shown). Since trypsin-activated PDE is soluble (Wensel & Stryer, 1986, Ong et al., 1989; Whalen & Bitensky, 1989; Catty & Deterre, 1991), these findings suggest that membrane-associated PDE can alter the release rate of light-activated transducin from the membranes, even in its $G_\alpha GTP\gamma S$-activated form.

A fit to the data in Figure 2, according to eq 8, gives a dissociation constant of $G_\alpha GTP\gamma S$–PDE interaction, $K_D = 8 \pm 4$ nM (SEM), and for the mole fraction of active $G_\alpha GTP_\gamma S$, $\rho' = 0.35$ (see Experimental Procedures). Reproduction with different preparations yielded an upper limit of 15 nM for the K_D. The fit is consistent with the following assumptions: (i) binding of the first G* to either of the two binding sites of a PDE molecule contributes equally to the PDE signal; (ii) binding of a second G* occurs with lower affinity, and its contribution to the PDE signal can be neglected (see Figure 5); (iii) $G_\alpha GTP\gamma S$ competes with light-activated G* for binding to both PDE binding sites.

The PDE Signal Is Stoichiometric with Respect to both Transducin and PDE. The amplitudes of both the dissociation signal and the PDE signal increase with the total amount of

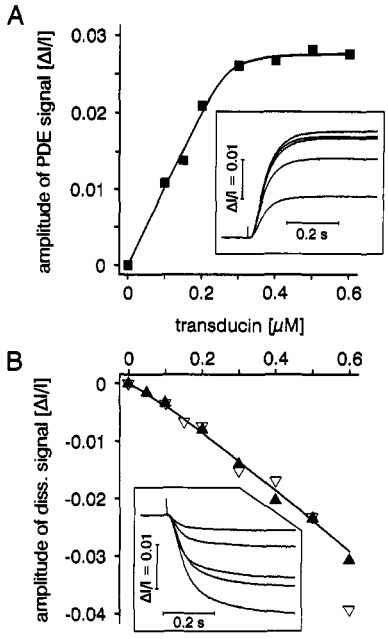

FIGURE 3: Dependence of the PDE signal and the dissociation signal on transducin concentration. (A) Amplitude of the PDE signal as a function of transducin concentration. The solid line is a fit according to eq 7 (see Data Analysis), yielding an apparent dissociation constant for G^*PDE_{mb} of K_D = 2.5 nM and a mole fraction of membrane-associated, active transducin of $\rho = 0.75$. Inset: PDE signals at 0.1, 0.2, 0.3, 0.4, and 0.5 μM transducin, respectively. (B) Amplitude of the dissociation signal as a function of transducin concentration. Different symbols identify different preparations (open triangles refer to the data shown in the inset). Inset: Dissociation signals at 0.1, 0.2, 0.3, 0.4, and 0.5 μM transducin, respectively. Measuring conditions: 3 μM rhodopsin (washed membranes), flash excitation $R^*/R = 2 \times 10^{-3}$, 500 μM GTP, 0.2 μM purified PDE (A), no PDE (B).

added transducin (Figure 3). By contrast to the dissociation signal (Figure 3B), the PDE signal shows a sharp saturation at a level related to the amount of PDE (Figures 3A and 4).

Excess transducin gives rise to additional, slower light-scattering changes, namely, (1) the slow ($t_{1/2}$ = 0.3–0.6 s) dissociation signal seen in the presence of preactivated PDE (see previous section) and (2) a slow ($t_{1/2}$ > 8 s) positive signal, which is probably the slow phase of the "phosphodiesterase activation signal" (PAS) (Bennett, 1986; Bennett & Clerc, 1992) and/or the PDE-dependent scattering signal described by Caretta and Stein (1985, 1986), and by Caretta et al. (1990). These signals are small below saturation (see Figure 1A,a), and the PDE signal can be separated by multiexponential fit (see Experimental Procedures). Above saturation, the slow components increase in approximate proportion to excess transducin, preventing exact evaluation of the PDE signal for high G_t concentration.

The saturation data in Figure 3 were fitted according to eq 7, yielding a value of 2.5 nM for the apparent dissociation constant K_D of the G*PDE–complex. For the mole fraction of membrane-bound, activatable transducin, one obtains $[G]_{mb} = 0.75[G]_{tot}$, which is in good agreement with previous findings (Schleicher & Hofmann, 1987; Bruckert et al., 1988). The data could not be fitted with the assumption of 100% activatable G* but higher K_D. The G_{tot}: PDE_{tot} molar ratio at the final level of the saturation curve varies among preparations of disk membranes, transducin, and PDE, respectively, between 1.5:1 and 4:1. This may indicate variations in the activity and/or membrane binding of the proteins. Values for K_D are between 0.1 and 2.5 nM, with membrane binding coefficients ρ = 0.25–0.75.

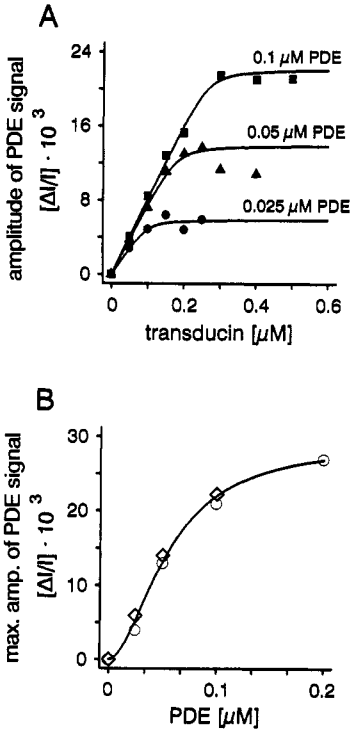

FIGURE 4: Dependence of the PDE signal on transducin and PDE concentration. (A) Amplitude of the PDE signal as a function of transducin concentration for different PDE concentrations. Measuring conditions: washed membranes (3 μM rhodopsin), flash excitation $R^*/R = 2 \times 10^{-3}$, 500 μM GTP, PDE concentration as indicated. The solid lines plot eq 7 with values of K_D = 1 nM (for all curves), ρ = 0.247 (0.025 μM PDE), ρ = 0.277 (0.05 μM PDE), and ρ = 0.373 (0.1 μM PDE), respectively. Since fixed $[PDE]_{tot}$ values (eq 7) were assumed, the deviations of ρ reflect the nonlinear dependence of the amplitudes on [PDE], as shown in (B). (B) Dependence of the maximal amplitude of the PDE signal (i.e., amplitudes in the presence of saturating amounts of transducin) on PDE concentration. Different symbols identify different preparations [diamonds represent data shown in (A)]. The solid line is a hyperbolic fit to the data.

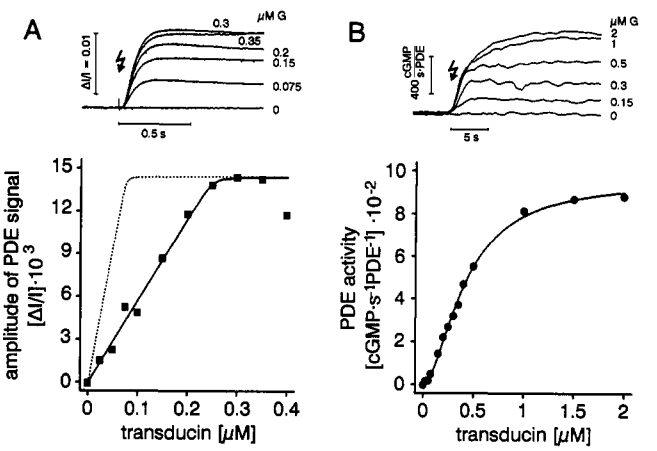

FIGURE 5: PDE signal and enzymatic PDE activity as a function of transducin concentration. Comparison of the light-scattering changes (A) with the light-induced PDE activity, measured as the pH change in the sample due to the enzymatic hydrolysis of cGMP (B) at various transducin concentrations. (A) Dependence of the PDE signal on transducin concentration. The solid line is a fit according to eq 7 (see Data Analysis) yielding values for K_D = 0.1 nM and ρ = 0.3. The dotted line gives the transducin concentration dependence of the PDE signal after the correction $G_{mb} = 0.3G_{tot}$. (B) Dependence of the PDE activity on transducin concentration. Traces are the derivatives of pH electrode readouts. Note that both the time scale and the range of concentration are different in (A) and (B). Measuring conditions: washed membranes (3 μM rhodopsin), flash excitation $R^*/R = 2 \times 10^{-3}$, 0.075 μM PDE, 500 μM GTP. cGMP (3 mM) was only added in case of measurements of PDE activity, since the PDE signal is superimposed on a cGMP-dependent slow signal (Caretta & Stein, 1986), which masks the PDE signal for high cGMP concentration.

When the transducin titration of the PDE signal (protocol of Figure 3) is repeated with different amounts of PDE (Figure 4A), the amplitude of the signal at saturation is stoichiometrically related to PDE_{tot}. A plot of the final level of each titration *vs* $[PDE]_{tot}$ is shown in Figure 4B.

Comparison of the PDE Signal with Enzymatic PDE Activity. In order to relate the PDE signal to enzymatic PDE activity, both PDE enzymatic activity and the PDE signal were titrated by the addition of transducin. Figure 5 shows that at saturation of the PDE signal (0.3 μM transducin) PDE activity is far from its maximal light-induced level (V_{max}). In contrast to the PDE signal, PDE activity follows a sigmoidal curve approaching saturation at a G:PDE molar ratio >30:1. The maximal activity under these conditions was approximately 1000 cGMP·PDE^{-1}·s^{-1}, in agreement with published results (Sitaramayya et al., 1986; Deterre et al., 1988; Bennett & Clerc, 1989).

A more detailed evaluation of the data in Figure 5 shows that maximal PDE activity is reached within 2–10 s after the flash. During this time, even the previously soluble proportion of transducin (G_{sol}) interacts with R* (Schleicher & Hofmann, 1987). Thus, PDE activity depends on the total transducin pool (G_{mb} and G_{sol}), while only G_{mb} can contribute to the PDE signal. Correction of the saturation curve by $[G]_{mb} = \rho[G]_{tot}$ (see previous section and Experimental Procedures) yields the dotted curve shown in Figure 5.

This curve saturates at approximately 10% of the maximal PDE activity, which may suggest that the relative enzymatic activity of the partially active G*PDE complex in the presence of membranes is about 10% of the maximal PDE activity attributed to the G^*_2PDE complex, as reported by Bennett and Clerc (1989; 5–10%), Whalen and Bitensky (1989; 10–20%), and Whalen et al. (1990; 5%). However, we cannot exclude more complex influences. For example, enhanced membrane binding of PDE due to its interaction with G* (Malinski & Wensel, 1992; Catty et al., 1992) could affect the activity assay. In addition, measurements of PDE activity cannot clearly differentiate between the various pools of activated PDE (G^*PDE_{sol}, G^*PDE_{mb}, $G^*_2PDE_{sol}$, and G^*_2-PDE_{mb}). Although we can therefore not fully analyze the relationship between PDE signal and PDE activity, the qualitative difference both in shape and in saturation of the titration curves remains. This difference excludes that the PDE signal monitors fully active PDE. The most active form of PDE is the membrane-bound complex of the enzyme with two G* ($G^*_2PDE_{mb}$) (Phillips et al., 1989; Bennett & Clerc, 1989; Malinski & Wensel, 1992). Since the PDE signal reflects membrane-bound PDE and the measured activity is so low at saturation, we cannot assign the PDE signal to the formation of the fully active $G^*_2PDE_{mb}$ complex. The results are consistent with the interpretation of the PDE signal as a monitor of the formation of the partially active G^*PDE_{mb} complex.

Interaction of G with PDE within 10 ms after Light Absorption.* In order to investigate the kinetics of G*–PDE interaction, we compared the dissociation signal and the PDE signal. Two parameters characterize the kinetics: (1) the slope, i.e., the slope of the tangent at the inflection point, normalized to the final amplitude; (2) the delay time, i.e., the time after the flash where this tangent intersects the base line (Figure 6B).

The slope of the dissociation signal yields a lower limit for the rate at which membrane-bound transducin is activated.

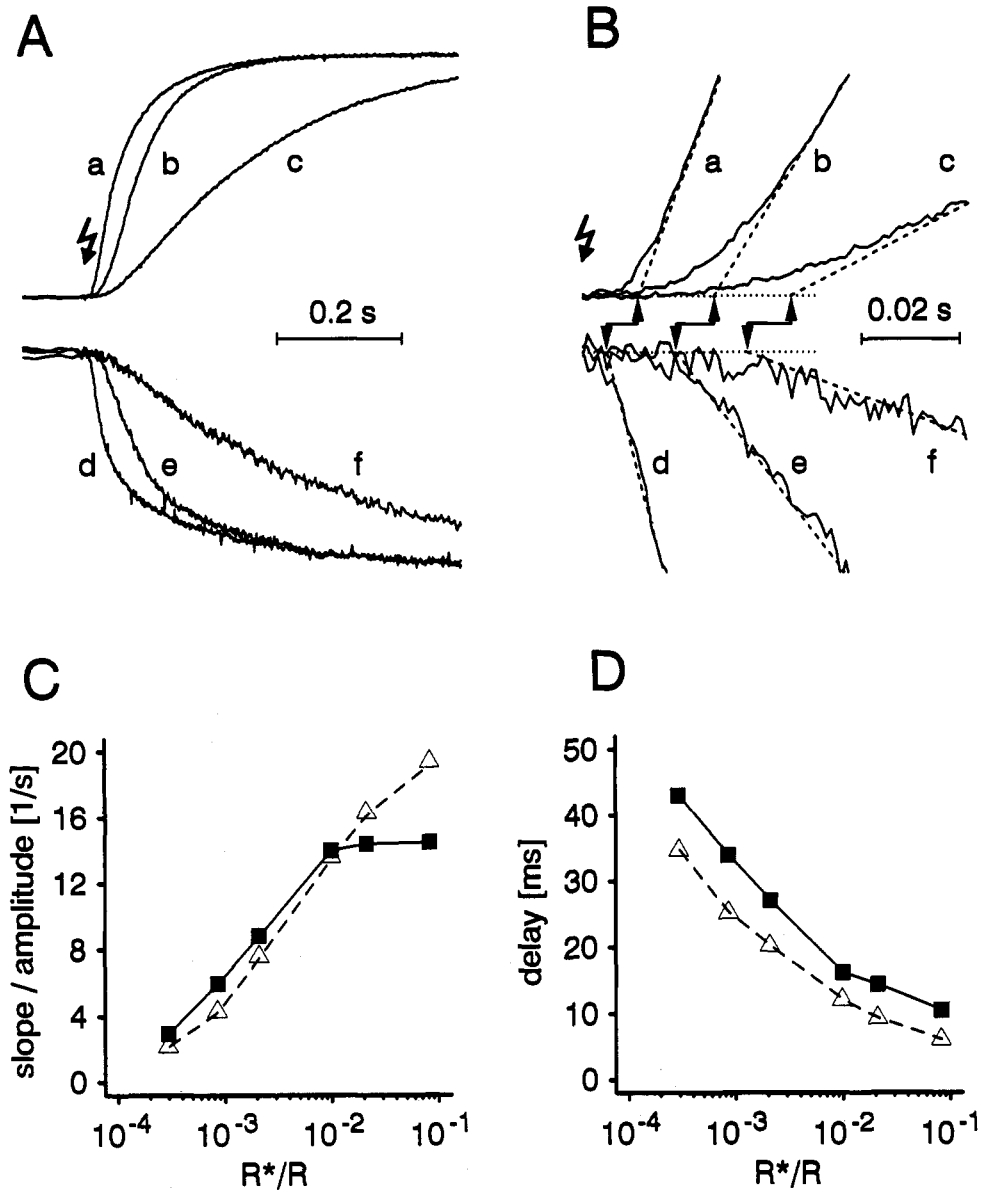

FIGURE 6: Kinetic analysis of PDE signal and dissociation signal. (A) PDE signals (traces a–c) and dissociation signals (traces d–f) induced by flashes of intensity $R^*/R = 8.4 \times 10^{-2}$ (a, d), 2×10^{-3} (b, e), and 3×10^{-4} (c, f). The signals were normalized to their final amplitude for better kinetic comparison. For intense flashes, the N-signal was subtracted (Schleicher & Hofmann, 1987). Measuring conditions: 3 μM rhodopsin (washed membranes), 0.4 μM purified transducin, 1 mM GTP; (a, b, c) 0.3 μM purified PDE, (d, e, f) no PDE. (B) Replot of the signals shown in (A) on expanded scales. Two parameters were used to characterize the kinetics of the signals, namely, (1) the slope, i.e., the slope of the tangent at the inflection point (dashed lines) normalized to the final amplitude; (2) the delay time, i.e., the time after the flash where this tangent intersects the base line (arrows). Delays belonging to the same intensity are indicated by horizontal lines. (C) Dependence of the relative slope of the PDE signal (squares) and the dissociation signal (triangles) on the fraction of photoexcited rhodopsin (R^*/R). (D) Dependence of the delay times of the PDE signal (squares) and the dissociation signal (triangles) on the fraction of photoexcited rhodopsin.

At low R^*, the dissociation signal and the PDE signal display the same slope, because the rate at which G* is formed limits its interaction with PDE. With increasing R^*, both signals are accelerated in parallel (Figure 6C). For large fractional bleaches ($R^*/R > 1\%$), the slope of PDE signal saturates sharply, indicating that now the G*–PDE interaction becomes rate-limiting (Figure 6C). Beyond this qualitative result, reaction rates cannot be determined, because they depend on the size of the G_t pool contributing to the signal, which cannot be determined with certainty.

The delay of both the dissociation signal (t_{diss}) and the PDE signal (t_{PDE}) shortens with increasing R^* (Figure 6D). The difference $t_{PDE} - t_{diss}$ between the delays is almost independent of R^* over the range tested. The relative delay $t_{PDE} - t_{diss}$ = 5–8 ms sets an upper limit to the time interval between dissociation of G* from rhodopsin and interaction with the first binding site on PDE. The short interval excludes an aqueous route for G*, since binding of a soluble protein to membranous binding sites takes considerably longer under the conditions (e.g., 1 s for membrane binding of soluble G_t; Schleicher & Hofmann, 1987).

The delay of the PDE signal extrapolates for intense flashes to less than 10 ms. This time interval represents the irreducible total delay between photoactivation of rhodopsin and interaction of G* with PDE.

DISCUSSION

The PDE Signal Reflects the Interaction between Activated Transducin and PDE. The goal of this study was to provide a fast assay for the coupling of activated G-protein to its effector. According to the criteria tested, the "PDE signal" is a real-time monitor of the interaction between light-activated transducin (G*) and the PDE on isolated rod disk membranes.

By its biochemical assignment, the PDE signal can be used as a kinetic monitor, although a physical interpretation is not yet available.

*The PDE Signal May Monitor the Transition into the Partially Active Membrane-Bound G*PDE$_{mb}$ Complex.* Activation of PDE involves the sequential formation of the membrane-bound complexes G*PDE$_{mb}$ and G*$_2$PDE$_{mb}$, of which the latter is the fully active form of the enzyme (Phillips et al., 1989; Bennett & Clerc, 1989; Malinski & Wensel, 1992). The PDE signal monitors the high-affinity interaction of G* with a single class of binding sites on PDE (linear dependence on transducin and sharp saturation, Figure 3), and at saturation, the enzymatic activity is less than half of the maximal light-stimulated level (Figure 5). The results are consistent with the interpretation of the PDE signal as a monitor of the transition into the partially active G*PDE complex on the membrane surface (G*PDE$_{mb}$). Below saturation of the PDE signal (Figures 3 and 4), most G* molecules formed by R* bind to PDE units; hence, they do not freely dissociate from the membrane. Titration with G* leads to an increasing level of G*PDE$_{mb}$ until the population of "first" binding sites on PDE is saturated by equimolar G*. Addition of excess transducin evokes the dissociation signal and a slower light-scattering change, which is related to the G*$_2$PDE complex (Caretta & Stein, 1986; Bennett & Clerc, 1992), but slower than its formation (Figures 1A,a and 5B).

*The G*PDE$_{mb}$ Complex Is Formed with K_D < 2.5 nM.* Among determinations of the apparent dissociation constant (K_D) from the titration of the PDE signal with transducin, most values were on the order of 0.1 nM, with an upper limit of 2.5 nM. A similar low K_D value was recently found with the energy-transfer interaction assay (Erickson & Cerione, 1991), and with the functional cGMP hydrolysis proton assay (Malinski & Wensel, 1992).

G Interacts with PDE$_{mb}$ in less than 5 ms.* The time course of G_t activation by R* is monitored with high fidelity by the dissociation signal (Kühn et al., 1981). The formation of the G*PDE$_{mb}$ complex, as monitored by the PDE signal, is delayed but otherwise identical in its time course (Figure 6A). After the delay, which comprises all precursor steps, G* and G*PDE$_{mb}$ rise in the early phase linearly with time (Figure 6B). This confirms the "delayed ramp" approximation, as predicted by Lamb and Pugh (1992). The PDE signal delay approaches 10 ms for sufficiently high *R** (Figure 6D), which gives an upper limit for the overall reaction time between rhodopsin photolysis and formation of G*PDE$_{mb}$. Analogous evaluation of the dissociation signal yields an upper limit of 7 ms for G* formation. The relative delay of G*PDE$_{mb}$ with respect to G* can be directly seen in Figure 6B,D. It decreases only 2-fold (from 10 to 5 ms) for a 500-fold increase of *R**. The relative delay sets an upper limit to the time an average G*, once formed, spends in diffusion, coupling to PDE, and formation of the complex. The actual process could well be faster, since we cannot exclude that part of the observed delay is due to the monitored structural change. In any case, it fits nicely into the irreducible total delay of 7 ms of the electrical response evoked by very intense flashes (Cobbs & Pugh, 1987). It is remarkable that this reaction, measured on a 1000-fold diluted, reconstituted system, has the same speed as in the functioning photoreceptor. Although the membranes are diluted, the interacting proteins seem to retain their density and collisional efficiency on the membrane.

The Interaction Occurs on the Membrane. The short interval between G* formation and its interaction with PDE reflects an effective coupling of G* to the PDE. This implies first of all that G* must not be released into solution, since under the conditions binding from solution to the membranous PDE would be more than 1 order of magnitude too slow (Schleicher & Hofmann, 1987). Actually, loss of G* from the membrane is observed, either if the PDE is blocked by $G_\alpha GTP_\gamma S$ or if there is an excess of G* over PDE; however, this loss is retarded (Figure 2) when PDE is bound to the membrane. The effect is sufficient to ensure effective kinetic competition of binding to the PDE. By this mechanism, G_t does not take the aqueous route, and a continuously membrane-bound interaction pathway from receptor to effector is established, in agreement with Liebman et al. (1987) and Uhl et al. (1990). Unfortunately, we cannot decide whether the membrane-bound path is realized in signal transducin *in situ*, as established for the related G-protein-coupled β-adrenergic system (Pfeuffer & Helmreich, 1975).

Open Questions. PDE slows the release of G* from the membrane, even in its $G_\alpha GTP\gamma S$-preactivated, thus noninteractive form (Figure 2). Membrane-bound PDE must exert an unknown effect on the membrane, which alters the membrane binding of G*. We may assume that membrane binding requires the intact holoprotein structure of G_t, even in its activated form, so that G* subunit dissociation would instantaneously release $G_\alpha GTP$ from the membrane. Under this assumption, $G_\alpha GTP$ cannot take a membrane-bound diffusion path to the PDE, and we are forced to conclude that G* interacts with the PDE as the holoprotein, forming a $G_{\alpha\beta\gamma}$–$PDE_{\alpha\beta\gamma\gamma}$ complex. This complex might represent the transient "switch" state, in which the high-affinity interaction between PDE_γ and $PDE_{\alpha\beta}$ is allosterically relieved (Sitaramayya et al., 1986; Deterre et al., 1988), preceding the formation of the fully active PDE complex.

These considerations relate to questions about the membrane and subunit interactions within the PDE complex, as raised in recent publications (Catty et al., 1992; Malinski & Wensel, 1992). Methods of specific modification and peptide competition are available for both the G_α and PDE_γ subunits (Cunnick et al., 1990; Brown, 1992; Artemyev & Hamm, 1992; Artemyev et al., 1992). It seems promising to combine these techniques with the flash photolysis assay described in this work. Structure–function studies on the R*G_t interaction have shown that kinetic monitoring can help to dissect sequential processes occurring during activation of a protein unit in signal transduction (Hofmann, 1993).

ACKNOWLEDGMENT

We thank Ulrike Walle, whose observations on rod outer segment preparations initiated this study, David Pepperberg for helpful discussions, and Markus Drechsler for electron micrographs. The technical assistance of Inge Bäumle is gratefully acknowledged.

REFERENCES

Artemyev, N. O., & Hamm, H. E. (1992) *Biochem. J. 283*, 273–279.

Artemyev, N. O., Rarick, H. M., Mills, J. S., Skiba, N. P., & Hamm, H. E. (1992) *J. Biol. Chem. 267*, 25067–25072.

Baehr, W., Devlin, M. J., & Applebury, M. L. (1979) *J. Biol. Chem. 254*, 11669–11677.

Bauer, P. J. (1988) *J. Physiol. 401*, 309–327.

Bennett, N. (1986) *Eur. J. Biochem. 157*, 487–495.

Bennett, N., & Clerc, A. (1989) *Biochemistry 28*, 7418–7424.

Bennett, N., & Clerc, A. (1992) *Biochemistry 31*, 1858–1866.

Bradford, M. M. (1976) *Anal. Biochem. 72*, 248–254.

Brown, R. L. (1992) *Biochemistry 31*, 5918–5925.

Bruckert, F., Vuong, T. M., & Chabre, M. (1988) *Eur. Biophys. J. 16*, 207–218.
Caretta, A., & Stein, P. J. (1985) *Biochemistry 24*, 5685–5692.
Caretta, A., & Stein, P. J. (1986) *Biochemistry 25*, 2335–2341.
Caretta, A., Stein, P. J., & Tirindelli, R. (1990) *Biochemistry 29*, 2652–2657.
Catty, P., & Deterre, P. (1991) *Eur. J. Biochem. 199*, 263–269.
Catty, P., Pfister, C., Bruckert, F., & Deterre, P. (1992) *J. Biol. Chem. 267*, 19489–19493.
Chabre, M., & Deterre, P. (1989) *Eur. J. Biochem. 179*, 255–266.
Cobbs, W. H., & Pugh, E. N., Jr. (1987) *J. Physiol. 394*, 529–572.
Cunnick, J. M., Hurt, D., Oppert, B., Sakamoto, K., & Takemoto, D. J. (1990) *Biochem. J. 271*, 721–727.
Deterre, P., Bigay, J., Robert, M., Pfister, C., Kühn, H., & Chabre, M. (1986) *Proteins: Struct., Funct., Genet. 1*, 188–193.
Deterre, P., Bigay, J., Forquet, F., Robert, M., & Chabre, M. (1988) *Proc. Natl. Acad. Sci. U.S.A. 85*, 2424–2428.
Erickson, J. W., & Cerione, R. A. (1991) *Biochemistry 30*, 7112–7118.
Fung, B. K.-K. (1983) *J. Biol. Chem. 258*, 10495–10502.
Fung, B. K.-K., Hurley, J. B., & Stryer, L. (1981) *Proc. Natl. Acad. Sci. U.S.A. 78*, 152–156.
Fung, B. K.-K., Young, J. H., Yamane, H. K., & Griswold-Prenner, I. (1990) *Biochemistry 29*, 2657–2664.
Hofmann, K. P. (1993) in *GTPases in Biology—Handbook of Experimental Pharmacology* (Dickey, B., & Birnbaumer, L., Eds.) Springer, New York (in press).
Hurley, J. B., & Stryer, L. (1982) *J. Biol. Chem. 257*, 11094–11099.
Kahlert, M., König, B., & Hofmann, K. P. (1990) *J. Biol. Chem. 265*, 18928–18932.
Kühn, H. (1984) in *Progress in Retinal Research* (Osborne, N., & Chader, G. J., Eds.) Vol. 3, pp 123–156, New York: Pergamon Press, New York.
Kühn, H., Bennett, N., Michel-Villaz, M., & Chabre, M. (1981) *Proc. Natl. Acad. Sci. U.S.A. 78*, 6873–6877.
Lamb, T. D., & Pugh, E. N., Jr. (1992) *J. Physiol. 449*, 719–758.
Liebman, P. A., & Pugh, E. N., Jr. (1979) *Vision Res. 19*, 375–380.
Liebman, P. A., & Evanczuk, A. T. (1982) *Methods Enzymol. 81*, 532–542.
Liebman, P. A., Parker, K. R., & Dratz, E. A. (1987) *Annu. Rev. Physiol. 49*, 765–791.
Malinski, J. A., & Wensel, T. G. (1992) *Biochemistry 31*, 9502–9512.
Ong, O. C., Ota, I. M., Clarke, S., & Fung, B. K.-K. (1989) *Proc. Natl. Acad. Sci. U.S.A. 86*, 9238–9242.
Pfeuffer, T., & Helmreich, E. J. M. (1975) *J. Biol. Chem. 250*, 867–876.
Phillips, W. J., Trukawinski, S., & Cerione, R. A. (1989) *J. Biol. Chem. 264*, 16679–16688.
Schleicher, A., & Hofmann, K. P. (1987) *J. Membr. Biol. 95*, 271–281.
Sitaramayya, A., Harkness, J., Parkes, J. H., Gonzalez-Oliva, C., & Liebman, P. A. (1986) *Biochemistry 25*, 651–656.
Smith, H. G., Jr., Stubbs, G. W., & Litman, B. J. (1975) *Exp. Eye Res. 20*, 211–217.
Stryer, L. (1986) *Annu. Rev. Neurosci. 9*, 87–119.
Tyminski, P. N., & O'Brien, D. F. (1984) *Biochemistry 23*, 3986–3993.
Uhl, R., Wagner, R., & Ryba, N. (1990) *Trends Neurol. Sci. 13*, 64–70.
Vuong, T. M., & Chabre, M. (1991) *Proc. Natl. Acad. Sci. U.S.A. 88*, 9813–9817.
Vuong, T. M., Chabre, M., & Stryer, L. (1984) *Nature 311*, 659–661.
Wagner, R., Ryba, N. J. P., & Uhl, R. (1987) *FEBS Lett. 221*, 253–259.
Wensel, T. G., & Stryer, L. (1986) *Proteins: Struct., Funct., Genet. 1*, 90–99.
Wensel, T. G., & Stryer, L. (1990) *Biochemistry 29*, 2155–2161.
Whalen, M. M., & Bitensky, M. W. (1989) *Biochem. J. 259*, 13–19.
Whalen, M. M., Bitensky, M. W., & Takemoto, D. J. (1990) *Biochem. J. 265*, 655–658.
Yamazaki, A., Bartucca, F., Ting, A., & Bitensky, M. W. (1982) *Proc. Natl. Acad. Sci. U.S.A. 79*, 3702–3706.